

NAVAL POSTGRADUATE SCHOOL

Monterey, California



**Demonstration of Linked UAV Observations and
Atmospheric Model Predictions in Chem/Bio Attack
Response**

Kenneth L. Davidson
Isaac Kaminer
Douglas Miller
Vladimir Dobrokhodov

Naval Postgraduate School
Monterey, CA

January 21, 2003

Approved for public release; distribution is unlimited.
Prepared for: NPS CDTEMS

20030326 002

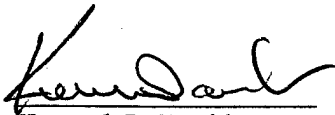
NAVAL POSTGRADUATE SCHOOL
Monterey, California 93943-5000

RADM David R. Ellison, USN
Superintendent

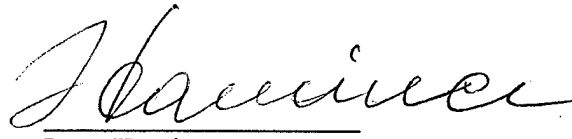
Richard Elster
Provost

This report was prepared for and funded by CDTEMS

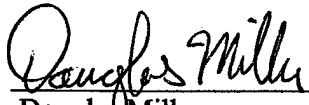
This report was prepared by:



Kenneth L. Davidson
Professor of meteorology



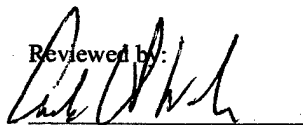
Isaac Kaminer
Associate Professor Aeronautics



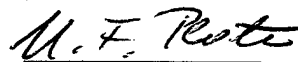
Douglas Miller
Research Assistant Professor of Meteorology



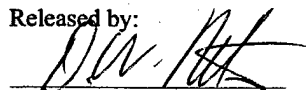
Vladimir Dobrokhodov
NRC Research Associate

Reviewed by:


Carlyle Wash
Chairman
Department of Meteorology
Naval Postgraduate School



M. Platz
Chairman
Department of Aeronautics
Naval Postgraduate School

Released by:


D.W. Netzer
Associated Provost and
Dean of Research
Naval Postgraduate School

REPORT DOCUMENTATION PAGE

Form approved

OMB No 0704-0188

Public reporting burden for this collection of information is estimated to average 1 hour per response, including the time for reviewing instructions, searching existing data sources, gathering and maintaining the data needed, and completing and reviewing the collection of information. Send comments regarding this burden estimate or any other aspect of this collection of information, including suggestions for reducing this burden, to Washington Headquarters Services, Directorate for Information Operations and Reports, 1215 Jefferson Davis Highway, Suite 1204, Arlington, VA 22202-4302, and to the Office of Management and Budget, Paperwork Reduction Project (0704-0188), Washington, DC 20503.

1. AGENCY USE ONLY (Leave blank)		2. REPORT DATE January 2003	3. REPORT TYPE AND DATES COVERED	
4. TITLE AND SUBTITLE Demonstration of Linked UAV Observations and Atmospheric Model Predictions in Chem/Bio Attack Response			5. FUNDING	
6. AUTHOR(S) Kenneth L. Davidson, Isaac Kaminer, Douglas Miller, and Vladimir Dobrokhodov				
7. PERFORMING ORGANIZATION NAME(S) AND ADDRESS(ES) Naval Postgraduate School Monterey, CA			8. PERFORMING ORGANIZATION REPORT NUMBER NPS-MR-03-001	
9. SPONSORING/MONITORING AGENCY NAME(S) AND ADDRESS(ES) N/A			10. SPONSORING/MONITORING AGENCY REPORT NUMBER	
11. SUPPLEMENTARY NOTES The views expressed in this thesis are those of the author and do not reflect the official policy or position of the Department of Defense or the U.S. Government.				
12a. DISTRIBUTION/AVAILABILITY STATEMENT Distribution Statement (mix case letters)			12b. DISTRIBUTION CODE	
13. ABSTRACT (Maximum 200 words.) Faculty and staff from the Departments of Meteorology and Aeronautics evaluated the integration of components for a near-real time decision aid designed to enable small units to respond in a focused way to a ChemBio attack. This effort included the field-testing of an atmospheric dispersion prediction model, an instrumented UAV for collecting meteorological data, and the means for linking the UAV data to real-time dispersion prediction. The primary modeling effort focused on an adaptation of the "Wind On Constant Streamline Surfaces" (WOCSS) model developed to run on a small computer with input from an external mesoscale model (MM5). The combined models were run for approximately one month for the region surrounding Camp Roberts, CA. In situ meteorological data were collected at the Camp Roberts airfield from 2 October to 5 November 2002 to validate the model predictions. The model results showed promise in capturing the diurnal evolution of near-surface temperatures that drive the local circulations in the warm season. Linking WOCSS with the atmospheric mesoscale model forecasts showed no significant improvement in wind forecasts when compared to the mesoscale model wind forecasts alone. Linking WOCSS to the trajectory visualization code revealed that vertical wind component estimates needed to be improved. The linked model/UAV demonstration of 7-9 October 2002 tested the synthesis of UAV measurements and dispersion model predictions. Although a UAV mishap occurred soon after the demonstration began, the instrumented UAV performance during this early period and in preliminary flight tests indicate that the hardware/software architecture for UAV data collection and its linkage with real-time dispersion prediction will be successful. Overall, the demonstration proved the feasibility of linking a coarse grid mesoscale model to a fine-scale diagnostic wind model for producing fine resolution forward and backward trajectories.				
14. SUBJECT TERMS			15. NUMBER OF PAGES 25	
			16. PRICE CODE	
17. SECURITY CLASSIFICATION OF REPORT Unclassified	18. SECURITY CLASSIFICATION OF THIS PAGE Unclassified	19. SECURITY CLASSIFICATION OF ABSTRACT Unclassified	20. LIMITATION OF ABSTRACT UL	

Abstract

Faculty and staff from the Departments of Meteorology and Aeronautics evaluated the integration of components for a near-real time decision aid designed to enable small units to respond in a focused way to a ChemBio attack. This effort included the field-testing of an atmospheric dispersion prediction model, an instrumented UAV for collecting meteorological data, and the means for linking the UAV data to real-time dispersion prediction. The primary modeling effort focused on an adaptation of the "Wind On Constant Streamline Surfaces" (WOCSS) model developed to run on a small computer with input from an external mesoscale model (MM5). The combined models were run for approximately one month for the region surrounding Camp Roberts, CA. In situ meteorological data were collected at the Camp Roberts airfield from 2 October to 5 November 2002 to validate the model predictions. The model results showed promise in capturing the diurnal evolution of near-surface temperatures that drive the local circulations in the warm season. Linking WOCSS with the atmospheric mesoscale model forecasts showed no significant improvement in wind forecasts when compared to the mesoscale model wind forecasts alone. Linking WOCSS to the trajectory visualization code revealed that vertical wind component estimates needed to be improved. The linked model/UAV demonstration of 7-9 October 2002 tested the synthesis of UAV measurements and dispersion model predictions. Although a UAV mishap occurred soon after the demonstration began, the instrumented UAV performance during this early period and in preliminary flight tests indicate that the hardware/software architecture for UAV data collection and its linkage with real-time dispersion prediction will be successful. Overall, the demonstration proved the feasibility of linking a coarse grid mesoscale model to a fine-scale diagnostic wind model for producing fine resolution forward and backward trajectories.

I. Background

Chemical and biological (ChemBio) weapon attacks have posed a response concern for some time and have gained a renewed focus. The toxic cloud has to be measured and its dispersion predicted to successfully respond to attacks by such weapons. This is a report of a model formulation, UAV configuration/instrumentation and field measurement effort to demonstrate and validate a method for the synthesis of measurements and predictions to aid in the response to an attack by chemical and biological weapons. The eventual goal of the demonstration/evaluation of integration of technology is to enable operational units to have a near-real time decision aid, integrated into a command and control net, to assist them in responding in a focused way to a ChemBio attack. This decision aid will be based on atmospheric model predictions of the agent transport and dispersion so that *effective* dispersion can be mapped upstream to the source or downstream to the region to be affected.

The multi-factor problem led to a demonstration attempt to sort out real issues and to calibrate expectations. The demonstration effort, addressing issues in ChemBio attack response, was of the transition of emerging as well as operational capabilities into seamless products based on

- 1) High resolution models for prediction and assimilation of dynamic atmospheric processes;
- 2) On-demand, near-continuous portable UAV sampling;
- 3) Capabilities in current remote (e.g. LIDAR) and in situ (e.g. tactical dropsonde) measurement of atmosphere; and
- 4) Open-ended information systems architecture.

In addition to the atmospheric modeling/UAV sampling value and linkage, the demonstration included in situ measurements for three evaluation/design reasons:

- 1) Value of mesoscale models for plume history and for initialization of conditions.
- 2) Value added to prediction by operational real-time collection of profiles, e.g. Tdrop or LIDAR, by other assets.
- 3) Value added by atmospheric sampling on UAV, and

Results from the demonstration will form the basis for future selection of several different types of models, data collection and model insertion procedures. One collection procedure is plume dimensions using UAV equipped with an appropriate sensor suite to measure the dispersed agent in the atmosphere. The project drew on resources that currently exist and are being (or soon will be) applied separately to operational descriptions of mesoscale circulation and air-land-sea interaction processes. Furthermore, the basic information system design is open-ended, which will allow the incorporation of advances in real-time data collection, distribution and modeling.

II. Approach/Procedures

The approach and procedures were selected to culminate with the IOP demonstration designed to simulate a "toxic" plume by releasing a smoker on the grounds of Camp Roberts, fly a UAV for mapping the dispersing plume, and having supporting atmospheric observations for evaluating assumptions and for ingesting into the atmospheric modeling parameter.

Atmospheric Modeling and measurement

Leading up to the October 2002 demonstration, a full physics mesoscale model was linked with the simple physics model (WOCSS) and post-processing code to create trajectories. The WOCSS model forms the operational basis for the prediction the origin and destination of the tracer plume given the UAV-mapped plume location and cross-wind structure. A demonstration of the capabilities completed over a period from 2 October through 5 November 2002, with an Intensive Operation Period (IOP) from 7 to 11 November 2002. During the 2 October through 5 November period, the model was run for a mesoscale region surrounding Camp Roberts, CA and in situ meteorological data collection were made at McMillan Airfield on Camp Roberts. For demonstration purposes, all atmospheric modeling components were self-contained on a SGI multiprocessor UNIX compute server located at the Naval Postgraduate School.



Figure 1. McMillan Airfield, Camp Roberts, CA

Atmospheric Modeling

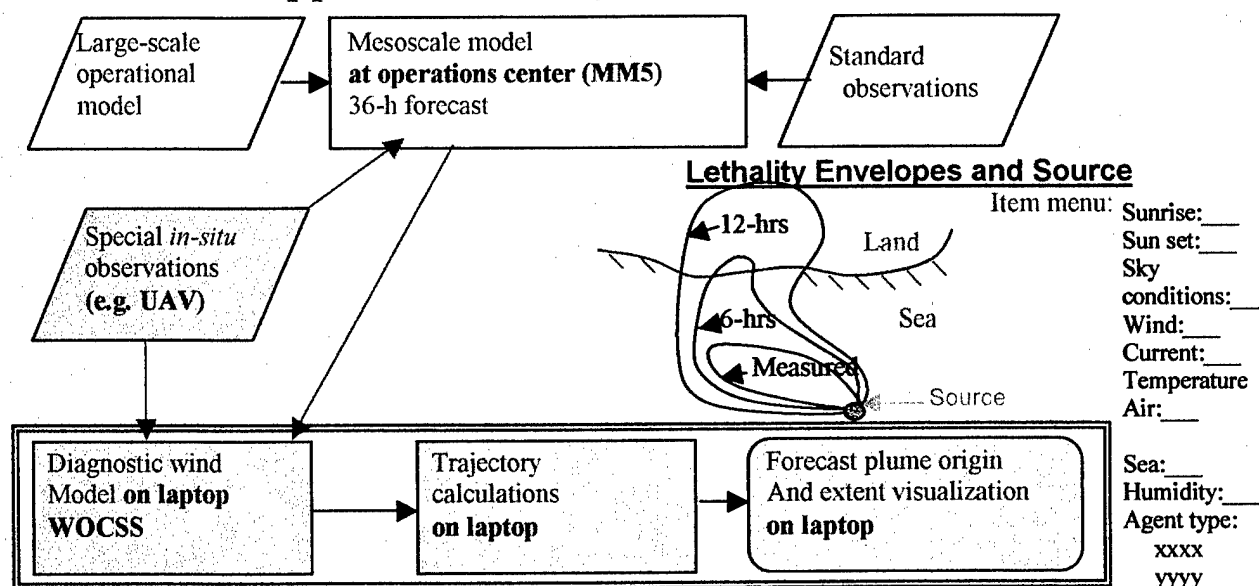
Because of the role of the atmosphere in the dispersion, an essential component in the demonstration is the measurement, analysis and prediction of its structure. The use of numerical models to predict weather is widespread. The class of models focusing on small-scale weather phenomena, known as mesoscale models, is commonly applied to plume dispersion. In a research mode, the mesoscale models have been run at horizontal grid spacing as small as 1 kilometer. In an operational setting, running models at such fine resolutions is impractical, since the computation time required is often greater than the lead-time of the forecast. Also, many of the model physics schemes were developed at a time when grid spacing were much larger and, hence, many of the simplifying approximations used in streamlining the code might not be applicable at fine resolutions.

Central to the methodology is a non-hydrostatic mesoscale model. The role of the mesoscale model is to transform information from large scales in a dynamically consistent fashion down to scales that are resolvable by the finest model grid domain. What is first required for successful implementation of the mesoscale model is the large-scale view of the atmosphere. A large-scale operational model was used as the first-guess with provisions for corrections based on standard observations (e.g. National Weather Service surface and upper-air observations) and "special" observations (e.g. aircraft data, remotely piloted aircraft data). How these various data sources are blended is important because, if they aren't combined in a way that the model "likes", information provided by them will be lost as the model establishes its version of proper dynamic and thermodynamic balance.

NPS/MR incorporated the Penn State/National Center for Atmospheric Research (NCAR) Mesoscale Model version 5 (MM5), which has been widely used for research programs sponsored by the Air Force, into the demonstration scenario, generating quasi-operational forecasts twice daily at the finest horizontal grid spacing of 9-12 kilometers. However, this model cannot be run on a field compatible laptop. Rather, output from these external location predictions were used to provide 4D data to the demonstrated field compatible trajectory model, Wind Over Constant Streamline Surfaces (WOCSS). Hence, the mesoscale model was linked both operationally and in research mode to a simple physics model (WOCSS) that has terrain elevation information at grid spacing of 100 meters. The overall linkage of models and measurement is shown in Figure 1.

The WOCSS-adjusted wind fields were used to compute trajectories that can characterize the past and future three-dimensional path of the toxic plume. The WOCSS horizontal grid scale is by no means limited to the 1-3 kilometer range in current use at NPS; rather, it is limited by the resolution of available terrain elevation information. A typical mesoscale model 36-h forecast requires 3-h actual wall clock time for completion which, when input to WOCSS requires 30 minutes to adjust the wind fields when model forecasts are output every three hours.

Approach: Atmospheric Modeling



Atmospheric numerical modeling flowchart

Figure 2 Atmospheric Modeling and Sampling Strategy

The full physics mesoscale model forecasts were output every 15 minutes over a large forecast volume and are converted into the format required by WOCSS to be defined for a smaller forecast demonstration location volume. One of the tested features was the WOCSS wind adjustment process. As the mesoscale model output frequency increases and the WOCSS horizontal grid scale decreases, the total WOCSS wind adjustment process increases beyond 30 minutes, dependent on the exact specifications of the WOCSS forecast volume. The WOCSS-adjusted three-dimensional wind fields were used as input for a trajectory code capable of deriving backward and forward trajectories from a defined location in space and time. An archive of re-adjusted WOCSS wind fields was maintained as in situ observations were received and used to correct WOCSS fields. The difference between the re-adjusted and original WOCSS wind fields serve as a basis for defining uncertainty in the predicted forward trajectories.

Atmospheric Measurement

The atmospheric measurement and data assimilation approach was to compare time and spatial scales of predicted and actual atmospheric properties that influence dispersion. With such attention to fine-scale atmospheric details, it was necessary to evaluate the suitability of initial prediction and to correct prediction errors that are typical in weather factors generated by any atmospheric model. The WOCSS-derived trajectories had to be validated by observations from an in situ collection of wind speed, direction, and temperature. A basic issue being addressed in the demonstration was whether assimilating the very latest observations within the region of the plume adds enough information to the best mesoscale vector wind profile and turbulent mixing estimates to justify the additional expenditure UAV time and resources.

In the demonstration mode, NPS/MR mounted a data collection/calibration/validation campaign on the boundary layer vector wind and turbulence-controlled mixing. NPS/MR performed data collection at the demonstration site. The collection was done with 3 ground-stations and 1 Rawinsonde system to apply to the time varying 3-D descriptions (i.e. 4D) of the test volume. The ground-station systems operated continuously during the entire time collection period with sensors listed in Table I-1 of Appendix I. The Rawinsonde system (Table I-2 of Appendix I) was used at scheduled times to collect profiles of vector winds, temperature, and humidity at pressure levels.

The continuous ground-based continuous measurements, schedule driven vertical profile measurements, provided measurements of the time and space separated atmospheric parameters that control dispersion and are required to initialize numerical models. The field collected data were those used to evaluate the suitability of and to correct the atmospheric forecasts as well as to update the toxic plume sampling and response strategy. With ground stations as well as sensors mounted aboard small unit deployed portable UAV's, everything just mentioned would be available in an operational mode.

To accomplish the in situ ground based continuous measurements, portable instrumented meteorological (Met) towers were installed on October 2, 2002 and in continuous operation until removed November 5, 2002. The tower designation and location are

- 1) **West Tower (SMOKE 1):** 35.72022 N, 120.77400 W, 275 m \pm 5.0 m
- 2) **East Tower (SMOKE 3):** 35.71651 N, 120.76275 W, 273 m \pm 6 m
- 3) **North Tower (SMOKE 2):** 35.72348 N, 120.76573 W, 300 m \pm 4.4 m

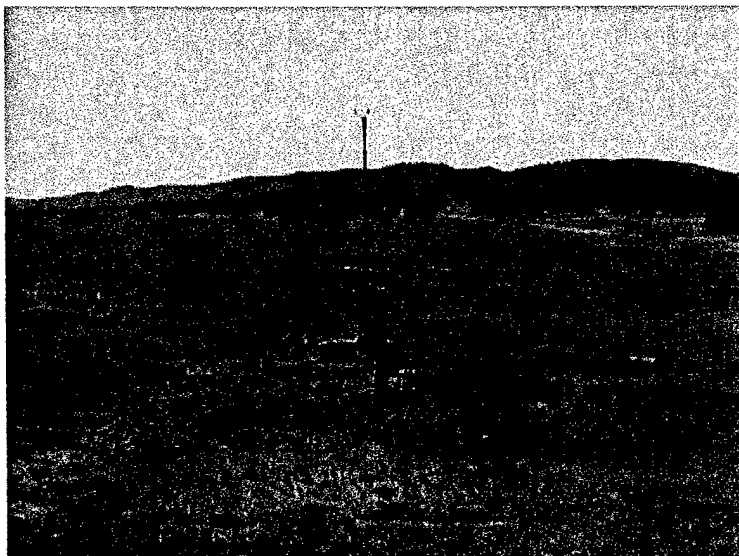


Figure 3. Instrumented portable meteorological (MET) tower installed at McMillan Field. Instrumentation listed in Table I-1 of Appendix I.

With regard to the location at McMillam Field demonstration site at Camp Roberts, the runway is oriented from SE to NW with a taxiway and hanger on the S side of the SE

end, Fig 1. Smoke 1, the west Met tower, was located about 50 ft south of the NW end of the runway. Smoke 2, the north Met tower, was located on hill several hundred feet North of the midpoint of the runway. Smoke 3, the east Met tower, was located about 50 ft north of the SE end of the runway

The towers were instrumented (Table 1, Appendix 1) for true vector wind (speed and direction reference to true North), air pressure, air temperature and humidity with identical sensors except that the West and North towers (SMOKE 1 and SMOKE 2) have temperature and humidity sensors at one level only whereas the East tower (SMOKE 3) has temperature and humidity sensors at two levels. The sensors were samples at 1 Hz and the output averaged over a two-minute interval.

All towers were instrumented with similar instruments except that the East Tower (Smoke 3) had Air Temperature and Humidity sensors in two levels instead of one

Wind Speed and Direction: Vaisala (Handar) 425S two-axis sonic anemometer

Air Temperature and Humidity: Rotronic HydroClip (Smoke 1 and 2, one level; Smoke 3, two levels)

Air Pressure: A.I.R. Barometer (AIR-DB-2A)

Sensors were sampled at 1 Hz and output averaged over 2-minute interval (five-minute interval after day 283) and identified with the UTC Date and Time. The output includes the following variables:

Data logger ID: Unique identification number

Time: UTC (Year, Julian Day, Hour-Minute)

True Wind Speed: m/s

True Wind Direction: degrees (meteorological convention)

Air Pressure: pressure – 1000 millibars

Air Temperature: °C

Relative Humidity: %

Battery: data logger supply voltage

Significant changes/events after the initial setup of the Met Towers was on October 2, 2002 were as follows:

- Vaisala Sonic anemometer on SMOKE 1 (West Tower) was replaced with RM Young Wind Monitor (prop-vane type) on October 8 (day 281) due to erratic performance of Vaisala instrument.
- RF links to towers was installed morning of October 9, 2002 (day 282).
- Collection interval changed from two-minute average to five-minute average on October 10, 2002 (day 283)
- Towers taken down and removed from McMilliam field on November 5, 2002 (day 339).

Upper-air measurements

Vertical profiles of meteorological properties were obtained with balloon launched and parachute descending and Kite-borne radiosondes. The launch location was 35.72 N, 120.76 W, at 273 m above sea level. Equipment involved in this is listed in Table I-2, Appendix I.

A summary of the launch times and sounding types are as follows:

Table 1 Vertical Profile Sampling: Camp Roberts CA		
Date	Launch Time (UTC)/PDT	Measurement method
8 Oct 02	1800/1000	Up/down rawinsonde
9 Oct 02	2138/1338	Balloon tethered sonde
9 Oct 02	2207/1438	Up/down rawinsonde
9 Oct 02	2256/1456	Balloon tethered sonde
10 Oct 02	1428/0628	Up/down rawinsonde
10 Oct 02	1551/0751	Up/down rawinsonde
10 Oct 02	1731/0931	Balloon tethered sonde
10 Oct 02	1656/0856	Up/down rawinsonde
10 Oct 02	1812/1012	Up/down rawinsonde

Up/down and balloon tethered rawinsondes were launched from a site near the mid-point of the runway at times before, during, and after UAV sampling. With up/down rawinsondes, data is received from the sonde both during a balloon-ascent and a parachute descent. This provides a better characterization of low altitude atmospheric conditions than with an ascending rawinsonde. It also, provides a three dimensional description of the fields since location is known due to the GPS or Loran navigation inherent in the vector wind determining component of the system. The spatial separation of these profiles will depend on sonde trajectories due to the ambient wind encountered.

The sonde and its parachute were released from the balloon using a timer-release mechanism. The timer was set to release the sonde at an altitude of about 1 km for the first launch of each day, at which point it descended by parachute back to the surface. This height was more than ample to characterize the low altitude atmospheric conditions affecting dispersion and for evaluation of the mesoscale model. Release heights of following rawinsonde flights were set based on an analysis of the profile data from the previous sounding. Additional balloon-borne (tethered) rawinsondes profiles of the near-surface atmosphere (up to about 50 m) were performed through out the collection as weather and time conditions permitted. These kite-borne sondes should provide a direct measurement of the near surface thermal structure, and thus details of the buoyancy influenced dispersion. The mesoscale models address properties at these scales.

NPS/MR also evaluated the UAV weather (met) observations for model application with regard to spatial and temporal accuracy. Meteorological observations from the UAV's that directly impact the atmospheric modeling effort are wind speed, direction, temperature, location (altitude, pressure, and latitude/longitude), and time

UTC). However, the primary one is wind speed and direction. The sampling frequency of the UAV is far beyond what is useful for a modeling comparison; so temporal averaging of the observations was required. Tolerable errors in observations of the atmospheric parameters were considered to be 1.0 m s^{-1} , 1.0° , 1.0 K , 5.0 m , 1.0 millibar , 0.005° , and 5.0% for wind speed, direction, temperature, altitude, pressure, latitude/longitude, and relative humidity, respectively.

UAV Instrumentation, Data Collection and Processing

Figure 4 represents the planned architecture for the UAV – ground station hardware. Preparation and testing for the demonstration was based on this set-up. The UAV was the Bai Tern (renamed a Frog) with 10.5' wingspan and 75 pound maximum takeoff weight. The data was collected by the onboard data acquisition system and transmitted to the ground station via serial RF modem. In operational modes, the Data Acquisition and Processing Computer on the ground will do all the necessary data processing to provide the Meteorology Code with the rewired data message, averaged over a pre-specified time interval. For this demonstration, the UAV pilot flew the aircraft. Additional guidance cues to the pilot will be developed as necessary.

UAV Frog had sensors shown in Figure 4 , which, in more detail, were:

- Navigation: Trimble AG132 differential GPS with 10Hz output and about 30cm rms error. The altitude is usually good to about 10 feet, which is better than our barometer altimeter.
- Meteorology: Vaisala HMM211 - Humidity 0-90% to 1%, 2% from 90-100% and 0.1C temperature accuracy.
- Communication Link: Freewave modem with 20 mile line of sight range at 115KBaud

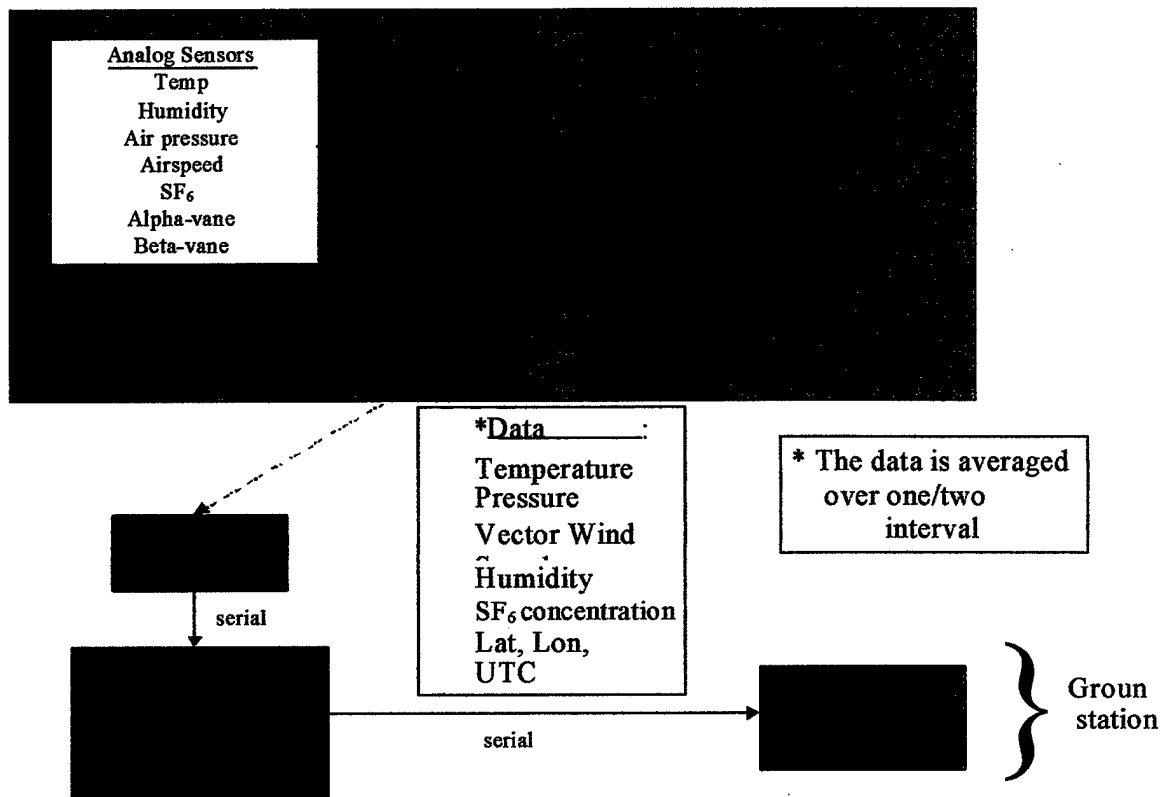


Figure 4 FROG Hardware and connectivity

III. Results

Atmospheric Measurement and Modeling results

a) Atmospheric Measurements

Time series of tower-based measurements (from 2 October to 5 November) and rawinsonde and kit-borne sonde profiles (on 10 and 11 October) appear in Appendix I. Significant feature of the time series are the diurnal variations of vector wind, temperature, and humidity as shown for the week of the demonstration, 9-15 October, where)) is 1600 PST. The dispersion trajectory altering wind speed variation and direction reversal can be seen in the barbs in the upper panel. The dispersions diffusion altering influence of temperature and relative humidity is shown in the lowest two panels. In general, the demonstrations occurred during times when atmospheric sampling and dispersion predictions would have been important in ChemBio attack response. These variations were captured at the three towers because of the continuous, multi-parameter sampling. Operationally, the atmospheric data would be collected on the UAV.

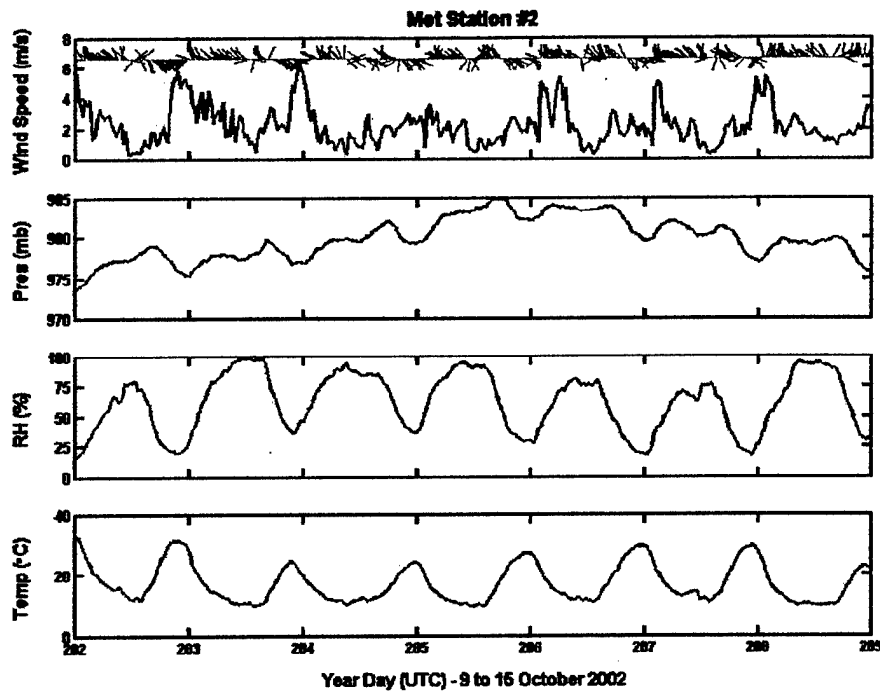


Figure 5. Seven- day (9-15 October) time series of surface layer (3 meter level) vector wind, pressure, RH and temperature during demonstration at McMillan Field, Camp Roberts CA. IOP occurred on 9-10 October.

Significant features of the profiles, over the nearly 24 hours of sampling, were the variation over the course of the day, from morning (1812 UTC = 1012 PST) to afternoon (2207 UTC = 1407 PST), of the layer immediately about the surface. It showed the difference in mixing volume and in the difference of vector wind profiles between the morning and the afternoon.

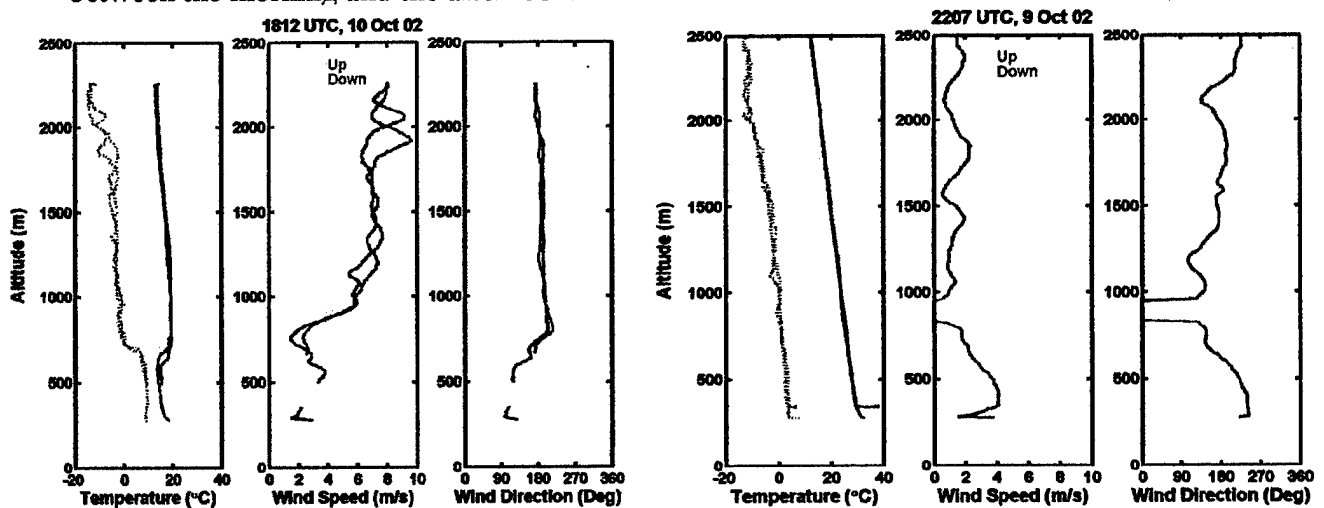


Figure 6. Profiles: Temperature and Dew Point Temperature, Wind speed and Direction for morning (1812 UTC) and afternoon (2207UTC) up-down radiosonde launches
Atmospheric modeling

The model forecast trajectories relevant to the day of the UAV flight are displayed in Figure 7. The model simulation started at 00:00 UTC 9 October (5:00 pm local time on 8 October) shows an almost half-circle trajectory path in Fig. 7 for air parcels released at 100, 500, and 1000 m above the ground over Camp Roberts at 00:00 UTC to their endpoint 36 hours later at 12:00 UTC 10 October. The simulated parcel paths show general ascent over the 36-hour period so that they have all been lifted at or above 1500 m above the ground by 5:00 am PDT 10 October. The model simulation started twelve hours later (5:00 am local time) shows that local weather conditions had changed enough so that the simulated parcels traveled a significantly farther distance from the Camp Roberts point of origin. These parcels experience larger overall ascent rates than seen with the earlier simulation so that by the end of the 36 hour period, the parcels range in altitude from 1500 to 2500 m above the ground.

With regards to a potential Chem/Bio attack, the simulated conditions suggest a slower cloud dispersion over the local Camp Roberts area for an agent released at 5:00 pm 8 October than if it were released twelve hours later. However, the parcel closest to the ground elevates quicker for the 5:00 pm launch than for the launch at 5:00 am on the following day. This is due, in general, to the lower atmosphere being less stable when the ground is warm and, with initial lift, a parcel will quickly rise above the ground.

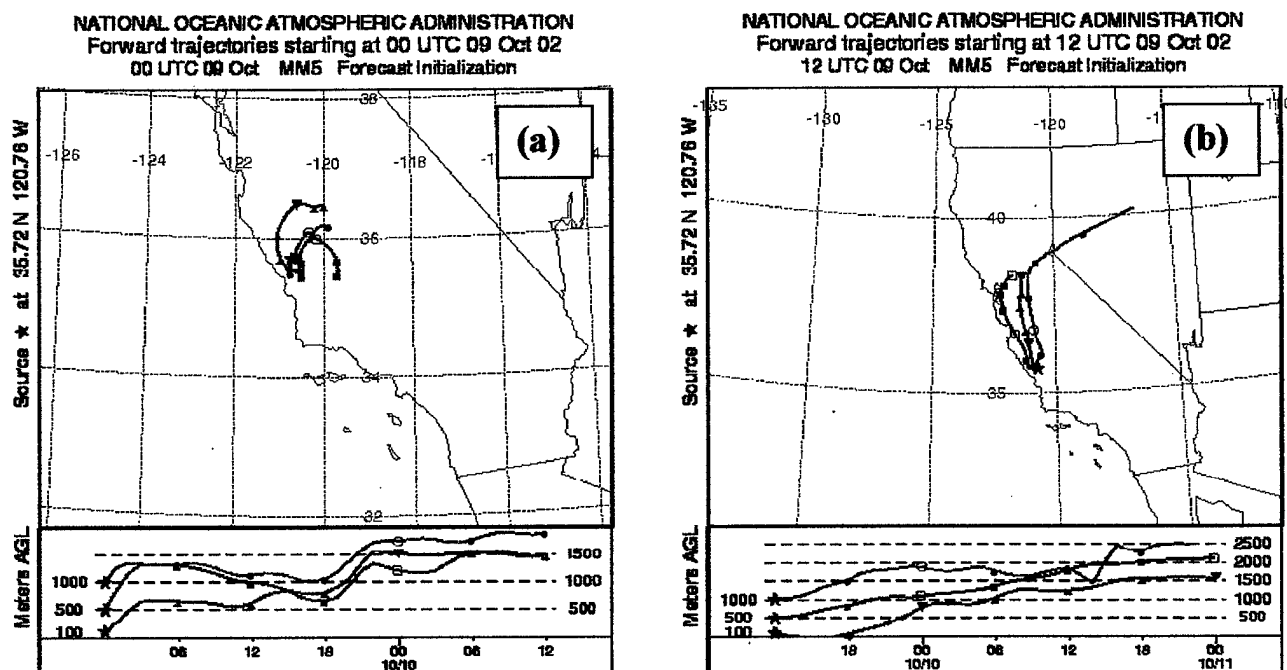


Figure 7. Model simulated trajectories for an air parcel located 100 (red), 500 (blue), and 1000 (green) meters above the ground at Camp Roberts for a simulation initialized at (a) 5:00 pm PDT 8 October and (b) 5:00 am PDT 9 October 2002.

Time series plots at the location of the North Tower meteorological ground station is shown in Figure 8. The red, blue, and green curves correspond to observations, MM5

predictions, and WOCSS predictions, respectively. The temperature series (Fig. 8 a) illustrates a common shortcoming of mesoscale models, they tend to simulate a smaller diurnal temperature variation than what is actually observed. Over this particular 36 hour simulation period from 5:00 pm 8 October to 5:00 am 10 October, the nighttime temperatures are never cold enough and the daytime temperatures are never warm enough compared to the observations.

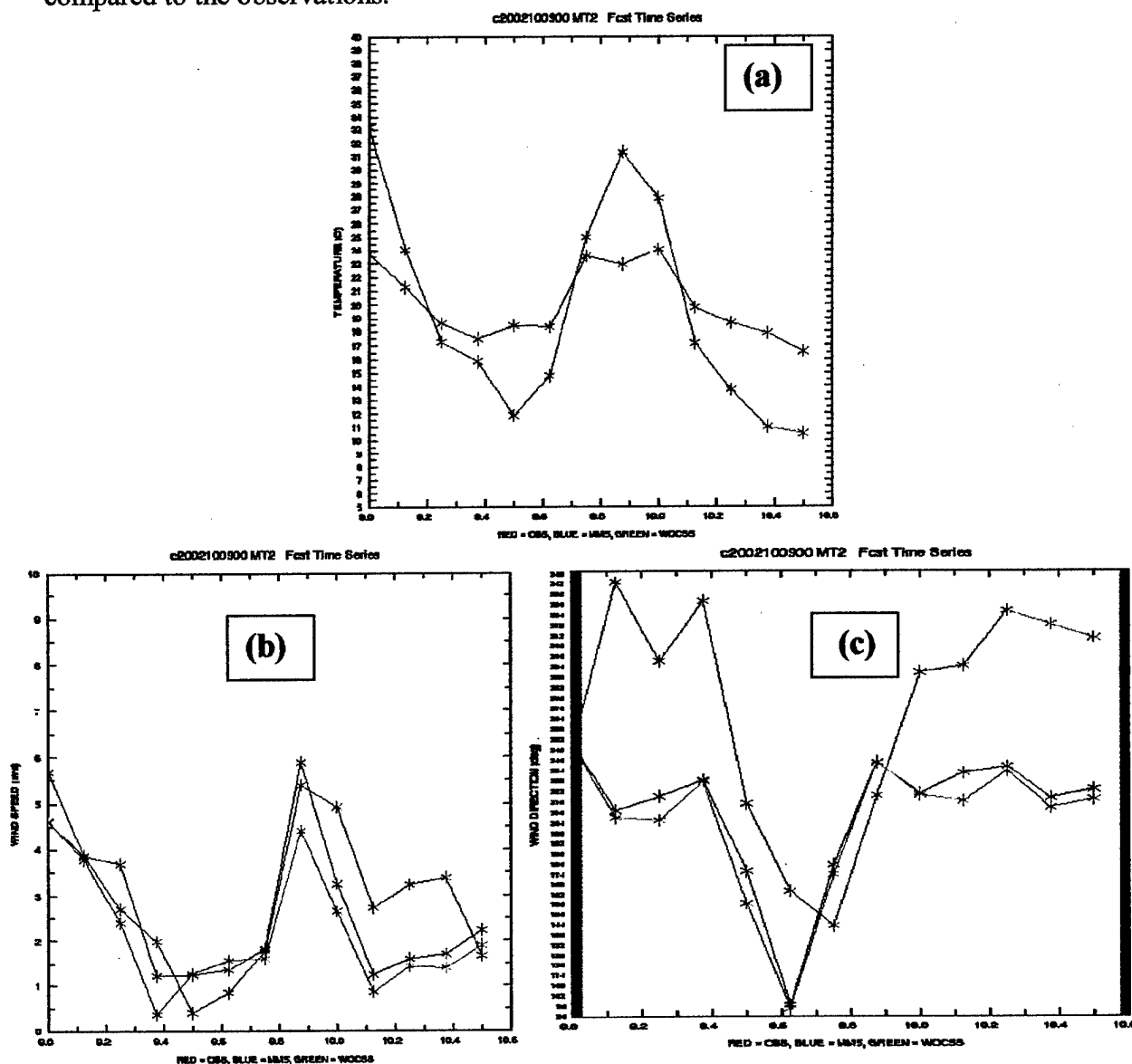


Figure 8. Observed and predicted (MM5 and WOCSS) (a) temperature, (b) wind speed and (c) direction from 10/09/00:00 UTC to 10/10/12:00 UTC.

The time series of wind speed (Fig. 8b) and direction (Fig. 8c) show a fairly respectable comparison between the models and what was observed. The observed winds never exceeded speeds of 6 m s^{-1} and this agreed with the model simulations. The greatest surface winds were observed and predicted to occur during the warm part of the day

while the weakest winds occurred during the cool part of the day. The condition of generally weak winds through the 36-hour period makes comparison of the wind direction traces difficult to interpret. In general, the model simulations suggested a southerly component while observations show a northerly component during weak wind speed periods. It is possible that the coarse mesoscale model grid spacing is unable to resolve local cold air drainage flows that could be giving the poor wind direction prediction results during the cool part of the day.

The diagnostic wind model (WOCSS) results don't show significant improvement compared with the coarse mesoscale model results for the Camp Roberts test domain. This is an artifact of the test site being an open flat basin, a good location for an airport. The WOCSS methodology is unnecessary for flat Battlespace environments and, under these conditions, is merely an interpolator of the larger-scale weather information. The benefits of the WOCSS methodology would be best demonstrated for operations over sites having peaks and valleys unresolved by the coarse horizontal grid spacing of the mesoscale model.

Examples of observed and predicted vertical atmospheric structure at 18:00 UTC (11:00 am PDT) for Camp Roberts are shown in Fig. 9 with the same color convention as in Fig. 8. The purple circles indicate the location of the vertical levels in the mesoscale model that set the limit on the resolvable vertical structure. The inability of the mesoscale model to warm the surface sufficiently is evident in the temperature sounding seen in Fig 9 a. The model also fails to simulate a strong temperature inversion (where temperature increases with increasing distance from the earth's surface) within the 300 to 500 m above ground level (AGL) layer. These atmospheric temperature inversions are important in that they trap pollutants within the layer of the atmosphere below them. Hence on this given day, a Chem/Bio agent released at this time near the ground at Camp Roberts would be trapped near the surface according to both the observations and the simulation.

Another result of the presence of an atmospheric temperature inversion is that the atmosphere within the layer near the surface is less likely to interact with the layer of the atmosphere above the inversion layer. In other words, the surface layer becomes decoupled from the atmosphere aloft. This is most evident in the wind profiles (Figs. 9 b and c) seen in the observed wind direction (Fig. 9c) shift evident in the 300 to 500 m AGL layer. This decoupling is missing in the model predicted wind directions, but is evident in the model predicted wind speed profiles (Fig. 9 b) in the form of a local wind speed maximum at about 620 m AGL. As stated previously, the WOCSS results don't show significant improvement over the coarse mesoscale model due to the Camp Roberts site being located in an open flat basin.

The observed and predicted wind soundings valid at 18:00 UTC 10 October (11:00 am PDT) suggest that a Chem/Bio agent released at Camp Roberts near the surface would initially drift northward along the Salinas Valley toward Salinas and the Bay area.

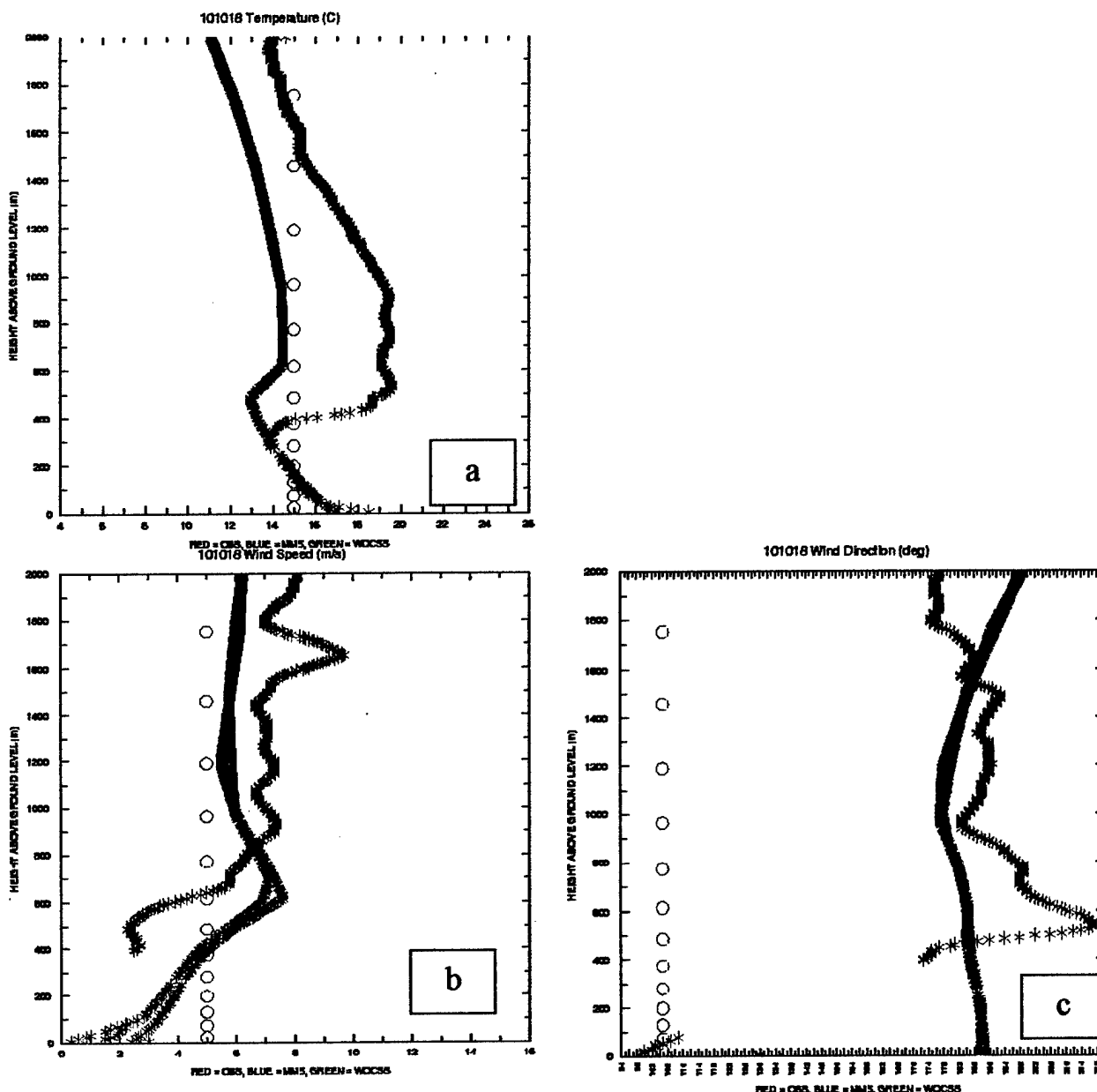


Figure 9. Observed and predicted (MM5 and WOCSS) (a) temperature, (b) wind speed and (c) direction profiles valid at 10/10/18:00 UTC (11:00 am PDT).

UAV Demonstration Results

The UAV principal eventual role in this project will be to both map the effective plume dispersion in the atmosphere and provide the wind estimation for the prediction of Chem/Bio agent dispersion. The present role was to make Meteorological observations that directly impact the atmospheric modeling effort is wind speed, direction, temperature, location (altitude, pressure, and latitude/longitude), and time (UTC). The sampling frequency of the UAV is far beyond what is useful for a modeling effort; so temporal averaging of the observations was required. A one- to two-minute average of atmospheric observations will be sufficiently useful for ingestion into the models. Tolerable errors in observations of the atmospheric parameters are 1.0 m/s, 1.0 deg, 1.0

K, 5.0 m, 1.0 millibar, 0.005 deg and 5.0 % for wind speed, direction, temperature, altitude, pressure, latitude/longitude, and relative humidity, respectively.

The UAV results of significance in this demonstration relate to wind comparisons. There are few types of data that determine spatial position of the UAV that is collected for the wind estimation purpose. Data of an air frame is represented by an air velocity and angles of attack and side-slip. Data measured in a body frame by the IMU sensor is represented by the accelerations, angular rates and magnetic vector variations. GPS data provides direct measurements of the coordinates, ground velocity and ground-tracking angle that are required for wind estimation model.

All the data about spatial position of the aircraft is used to solve simple dynamic task $\vec{W}^i = \vec{V}_{GPS}^i - R_b^i R_a^b \vec{V}_a$. Here \vec{W}^i - vector of wind velocity calculated in an inertial frame, \vec{V}_{GPS}^i - inertial velocity vector measured by GPS, \vec{V}_a - vector of air speed, R_a^b and R_b^i traditional rotational matrixes for the velocity transformation from air frame to body and from body frame to inertial one. Calculation of the rotational matrixes is based on the measurements provided by sensors described above. Prior to drive the model all incoming signals are calibrated and filtered to provide real efficiency of wind estimation.

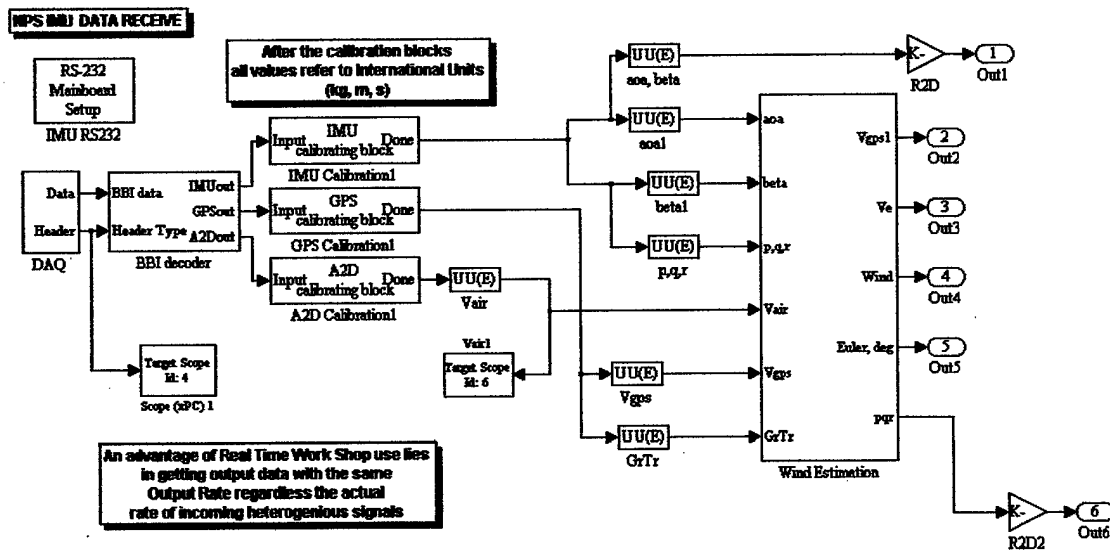


Figure 10. Real time processing model

The wind estimation model has been implemented in a Simulink environment. Real-Time Workshop tool provides an ability to execute this model in a remote computer in a real time. Entire model and their wind estimation subsystem employed are explicitly presented in next two figures.

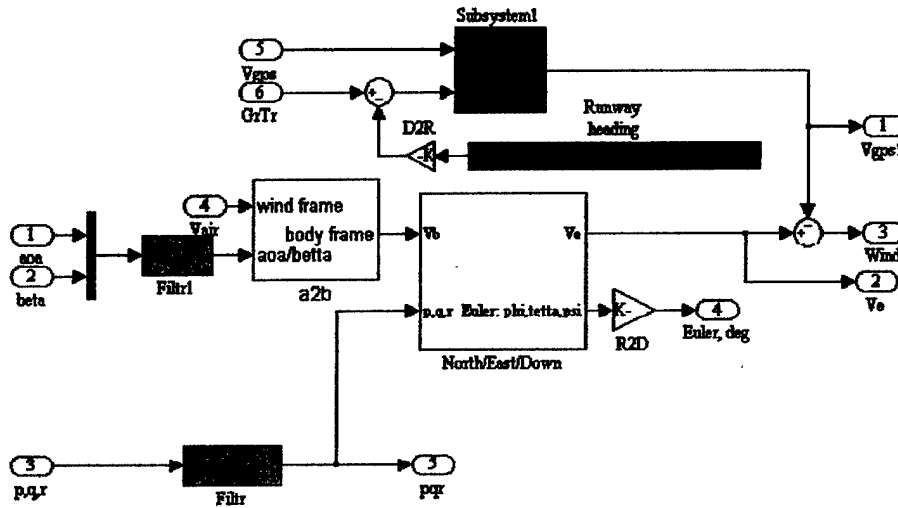


Figure 11. Wind estimation model

Fig 12 illustrates the quality of the obtained result. They present estimations of the wind direction and magnitude (left side) in comparison with data obtained traditionally (right side) from balloons. The real-time data looks much noisier due to high data acquisition rate. Optimal filtering UAV observed data would be a topic of study in follow-on demonstrations.

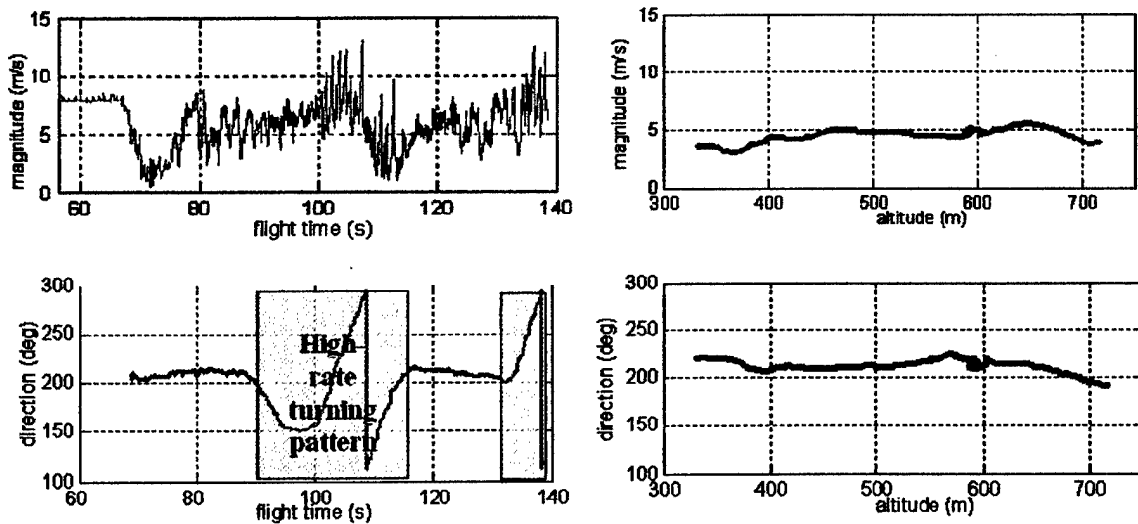


Figure 12. UAV FROG vector wind estimation results

A summary of the comparison of the averaged results as it was mentioned earlier is presented on final table, Table 2.

Table 2. Wind Statistics.	Wind magnitude	Wind direction
Real-Time model	» 6.5m/s	» 210 deg
In situ data	» 4.9m/s	» 214 deg
Error	» 1-3m/s	» 1- 5 deg

IV. Conclusions

The atmospheric mesoscale model results showed promise in capturing the diurnal evolution of near surface temperatures that drive the local circulations in the warm season. The model consistently underestimated the daytime heating at the ground and yet maintained a reasonable wind and atmospheric stability forecast. Trajectories based on model forecasts showed a reasonable path for the given large-scale conditions but were not verified. Future work would include incorporating observations into the model initialization to correct for the cold daytime temperature bias and examine the impact on successive temperature and trajectory forecasts. Another aspect worth future exploration is the quality of the model forecasts over a broader range of meteorological conditions, validating model performance for cold as well as warm season conditions.

Linking WOCSS with the atmospheric mesoscale model forecasts showed no significant improvement in wind forecasts when compared to the mesoscale model wind forecasts alone. This is an artifact of the test site being located in an open flat basin, where WOCSS essentially acts as an interpolator of the larger-scale weather information. An ideal future test would take place at a site having peaks and valleys unresolved by the coarse horizontal grid spacing of the mesoscale model. Linking WOCSS to the trajectory visualization code revealed serious shortcomings in the estimate of the vertical wind component that needs to be improved for future tests. Another avenue of future work will be to examine how incorporating actual observations into WOCSS will impact WOCSS-derived trajectory forecasts.

With regard to the UAV Frog performance in the demonstration, highly efficient meteorological and navigation information was obtained during the preliminary flight tests that proved the efficiency of the UAV in the demonstration. Developed hardware architecture has confirmed a concept of operations for a real-time data acquisition airborne unit to support meso-scale meteorological prediction. Currently employed hardware components provided a current state of the art in portability of UAV system deployment. The developed and demonstrated real-time software has showed its compatibility with real-time processing requirements, adequate accuracy and robustness. The analyzed results have revealed a significant potential and promising direction in UAV based system that should be further addressed.

Future work would include an improvement of hardware design that allows more flexibility in hardware rigging. It should support an exchangeable utilization of more precise and numerous heterogeneous sensors for the "full" variety of possible chemical agents and various needs.

Software enhancement should address two principal issues that allow moving the project onto direction of increased autonomy. The first topic includes an implementation of complimentary filtering technique to provide better resolution of the heterogeneous information from variety of possible sensors. The other issue should address the development and implementation of pilot support tools to extend the operational area and simplify the navigation task. It can be achieved by the development and implementation of such trajectory pattern (grid) where UAV is autonomously guided and also by employing a modern GPS based technique through the real-time visualization of navigational data.

Overall the demonstration proved the feasibility of linking a coarse grid mesoscale model to a fine scale diagnostic wind model for producing fine resolution forward and backward trajectories. Further, it demonstrated the most probable successful outcome of linking in situ UAV collection with the model prediction. This would support the forecast and potential sampling of dispersed agent. As mentioned above, several challenges were noted in the model prediction, which will provide future research opportunities to improve on the mesoscale model- diagnostic wind model methodology as a tool for defending against ChemBio weapon attacks. Another very important aspect of future work is the actual transition of WOCSS and the HYSPLIT visualization/trajectory code to a laptop for a portable capability and linking it to the UAV sampling. This study demonstrated that it was possible to transition to the field Laptop for modeling and to the UAV for necessary sampling.

APPENDIX I: NPS Measurement Systems

Parameter	Instrument	Installation Requirements	Physical Description
Wind Speed	RM Young Wind Monitor	Instruments mounted in well exposed location for good air flow characteristics	Instrument Assembly weighs 10 pounds measuring 2'x3"x6" mounted on 10 ft mast.
Wind Direction			
Air Temperature	Rotronics Temp/RH Probe		
Relative Humidity			
Data Logger	Campbell Scientific CR10X	Data logger mounted near AC power, within 100 ft of Instrument Mast	Data Logger Assembly weighs 20 pounds and measures 12"x14"x6"
Monitor	Laptop PC	PC located in operations space within 100 ft of Data Logger	Requires about 2 sq ft desk space

Table I-2. Rawinsonde Operations			
Rawinsonde System (1)		Installation Requirements	Physical Description
404 MHz rawinsonde Antenna		Antennae mounted high with good exposure	6 in dia x 5 ft typically rail mounted on 4 ft x 2" nominal dia. pipe
GPS rawinsonde Antenna			3" dia x 2" high rail mounted on 1" dia pipe
Rawinsonde Receiver		Rawinsonde Receiver and Monitor occupy approx 24"x 48" desktop space	MRS Receiver Weighs 70 lbs 18"x18"x24"
Rawinsonde Monitor	Laptop PC and Printer		PC ~ 5 lbs Printer ~10 lbs
Rawinsonde Expendables	Rawinsondes, Kites and accessories	Storage Required approx 10 cu ft. in operations areas Kites an accessories up 6 ft in length	
Balloon Launch Shelter		Located in exterior operations area	6 ft DIA x 4 ft high
Helium			2 – 5 cylinder storage near launch shelter
Operations Support: Spare Parts and Tools		Stowed unless failure	200 lbs, 20 cu ft

INITIAL DISTRIBUTION LIST

1. Defense Technical Information Center
8725 John J. Kingman Road, Suite 094
Ft. Belvoir, VA 22060-6218
2. Dudley Knox Library
Naval Postgraduate School
411 Dyer Road
Monterey, CA 93943-5101
3. Naval Postgraduate School
Research Administration (Code 09)
699 Dyer Road
Monterey, CA 93943-5001
4. Prof. D. Netzer, Code 09
Naval Postgraduate School
Monterey, CA 93943-5001
5. Prof. T. Lewis, Code CSLT
Naval Postgraduate School
Monterey, CA 93943-5001
6. Capt. Robert Clark, SPAWAR PMW 155
Space and Naval Warfare Systems Command
4301 Pacific Highway
San Diego, CA 92110-3127
7. Thomas Piwower, PMW
Space and Naval Warfare Systems Command
4301 Pacific Highway
San Diego, CA 92110-3127
8. Paul Tiedeman
Naval Sea Systems Command
Washington, DC
9. The Oceanographer of the Navy
United States Naval Observatory
3450 Massachusetts Avenue, NW
Building 1
Washington, DC 20932-5421

10. Dr. R. Ferek, code 322 MM
Office of Naval Research
800 North Quincy Street
Arlington, VA 22217-5660
11. CDR Julia Spinelli
DTRA TDOC
6801 Telegraph Road
Alexandria, VA 22310
12. Richard Benney
Airdrop Technology Team
Airdrop/Aerial Delivery Directorate
US Army Soldier, Biological & Chemical Command
ATTN: AMSSB-RAD-AT (N) (Benney)
Kansas St.
Natick, MA 01760-5017
13. Dave LeMoine
Airdrop Technology Team
Airdrop/Aerial Delivery Directorate
US Army Soldier, Biological & Chemical Command
ATTN: AMSSB-RAD-AT (N) (LeMoine)
Kansas St.
Natick, MA 01760-5017
14. Prof. Kenneth L. Davidson, MR/DS
Department of Meteorology
Naval Postgraduate School
589 Dyer Road, 254 Root Hall
Monterey, CA 93943-5114
15. Assoc. Research Professor Douglas Miller, Code MR/Z
Department of Meteorology
Naval Postgraduate School
589 Dyer Road, 254 Root Hall
Monterey, CA 93943-5114
16. Assoc Professor Isaac Kaminer, Code AA/KA
Department of Aeronautics and Astronautics
Naval Postgraduate School
Monterey, CA 93943-5114

17. Assoc Professor Richard Howard, AA/HO
Department of Aeronautics and Astronautics
Naval Postgraduate School
Monterey, CA 93943-5114
18. Vladimir Dobrokhodov, AA/OB
Department of Aeronautics and Astronautics
Naval Postgraduate School
Monterey, CA 93943-5114